1990

A spatial analysis of variance applied to soil-water infiltration

C Gotway
University of Nebraska

Noel A. Cressie
University of Wollongong, ncressie@uow.edu.au

A spatial analysis of variance applied to soil-water infiltration

Abstract

A spatial analysis of variance uses the spatial dependence among the observations to modify the usual interference procedures associated with a statistical linear model. When spatial correlation is present, the usual tests for presence of treatment effects may no longer be valid, and erroneous conclusions may result from assuming that the usual F ratios are F distributed. This is demonstrated using a spatial analysis of soil-water infiltration data. Emphasis is placed on modeling the spatial dependence structure with geostatistical techniques, and this spatial dependence structure is then used to test hypotheses about fixed effects using a nested linear model. -Authors

Keywords

applied, analysis, variance, infiltration, spatial, water, soil

Disciplines

Physical Sciences and Mathematics

Publication Details

Gotway, C. & Cressie, N. A. (1990). A spatial analysis of variance applied to soil-water infiltration. Water Resources Research, 26 (11), 2695-2703.

WATER RESOURCES RESEARCH, VOL. 26, NO. 11, PAGES 2695–2703, NOVEMBER 1990

A Spatial Analysis of Variance Applied to Soil-Water Infiltration

CAROL A. GOTWAY[1] AND NOEL A. C. CRESSIE

Department of Statistics, Iowa State University, Ames

A spatial analysis of variance uses the spatial dependence among the observations to modify the usual inference procedures associated with a statistical linear model. When spatial correlation is present, the usual tests for presence of treatment effects may no longer be valid, and erroneous conclusions may result from assuming that the usual F ratios are F distributed. This is demonstrated using a spatial analysis of soil-water infiltration data. Emphasis is placed on modeling the spatial dependence structure with geostatistical techniques, and this spatial dependence structure is then used to test hypotheses about fixed effects using a nested linear model.

1. INTRODUCTION

At a given location in the field the ability of water to infiltrate soil depends upon the existing soil-water distribution with depth, the rate of water application to the soil surface, and the soil-pore-structure distribution with depth. As the location varies across the field, this ability will vary spatially so that locations nearby are more alike with regard to infiltration than those far apart. This spatial dependence among the infiltration measurements may be used to enhance any statistical analysis of soil-water infiltration. Moreover, failure to account for spatial correlation, in general, can lead to erroneous inference procedures that could result in incorrect scientific conclusions.

In what is to follow we summarize the data, methodology, and results from the robust-resistant spatial analysis of soil-water infiltration data presented by *Cressie and Horton* [1987]. The spatial correlations among the soil-water infiltration measurements are modeled using geostatistical methods; kriging and cross-validation techniques are implemented to check and adjust for outliers. Finally, using a nested linear model with covariances determined by the modeled spatial correlations, various statistical hypotheses of interest are tested, and the consequences of overlooked spatial dependence are demonstrated.

2. EXPLORATORY SPATIAL DATA ANALYSIS OF SOIL-WATER INFILTRATION

The variable of interest in this study is soil-water infiltration, as measured with a double-ring infiltrometer apparatus. The double-ring infiltrometer is a device consisting of two concentric rings: the outer ring is used to stop the horizontal spread of the water so that only the vertical subsidence is measured, and the other is used to pond the water so that the infiltration rate can be measured. An experiment was conducted in the summer of 1983 to determine the effects of tillage treatment on soil-water infiltration. This experiment was performed using plots that were plowed in the fall of 1982 with the following tillage treatments: moldboard plow (15–20 cm), paraplow (25–30 cm), chisel-plow (15–20 cm), and no tillage. For more details, see *Mukhtar et al.* [1985] and *Cressie and Horton* [1987].

Water stage recorders were used to record the soil-water infiltration as a function of time [*Mukhtar et al.*, 1985]. For the part of the experiment of interest to us here, 30-min cumulative infiltration measurements (in centimeters) were made at 24 locations (on a 3 × 8 grid arrangement) within each of four plots. Two sets of infiltration measurements were obtained, one in May and one in July, but we will analyze only the July data here. Figure 1 [from *Cressie and Horton*, 1987] illustrates the arrangement of the spatial sites and the tillage treatments. Because of limited resources, only one block of a randomized block design was used for the spatial experiment. This design is unfortunate and makes any conclusions tentative since strictly speaking treatment and plot location are confounded; further details are given below. However, there are a number of instances in science where, even with unlimited resources, replicated designs are an impossibility, and comparison of properties among different units may still be desired (for example, comparison of lithological characteristics among rock units in a formation). At the very least the analysis that follows provides an illustration of a spatial analysis of variance.

To begin the spatial analysis of soil-water infiltration, the data in Figure 1 are written as

$$\{y_{ijk}: i = 1, 2, 3, 4, j = 1, 2, 3, k = 1, \cdots, 8\} \quad (1)$$

so that y_{ijk} is the kth observation in the jth column of treatment i. Set $i = 1$ for the moldboard tillage treatment, $i = 2$ for paraplow, $i = 3$ for chisel, and $i = 4$ for no-till. Using robust-resistant exploratory spatial data analysis procedures, *Cressie and Horton* [1987] show that in order to estimate the spatial dependence in the data a symmetrizing and variance stabilizing square-root transformation is needed, followed by subtraction of column medians to remove trend. Specifically, define

$$z_{ijk} = (y_{ijk})^{1/2} \quad (2)$$

$$r_{ijk} = z_{ijk} - \tilde{z}_{ij} \quad (3)$$

where $\tilde{z}_{ij.} = \text{med}\{z_{ijk}: k = 1, \cdots, 8\}$. The square-root transformation was applied so that on this scale, data can be written as a mean effect (made up of additive components of spatial location and treatment effects) plus a Gaussian random term. (For details, see *Cressie and Horton* [1987].) Figure 2 shows stem-and-leaf plots of the median-based

[1]Now at Sandia National Laboratories, Albuquerque, New Mexico.

Paper number 90WR01539.
0043-1397/90/90WR-01539$05.00

MOLDBOARD			PARAPLOW				CHISEL			NO-TILL		
31.55	27.90	12.50	7.54	36.64	26.47		10.24	8.93	14.77	4.30	9.75	9.49
31.10	35.45	6.84	5.40	38.82	42.02		6.81	8.55	11.84	6.10	13.41	14.84
38.05	53.25	13.90	13.43	10.67	20.33		3.99	1.83	7.96	4.48	15.38	10.41
17.62	39.04	18.15	26.49	30.28	35.20	→ N	7.10	4.65	5.32	8.67	15.29	12.10
8.64	34.14	28.53	39.82	27.52	39.65		2.12	5.29	8.31	3.54	12.56	20.59
6.65	23.30	25.97	20.19	25.15	44.42		6.02	3.52	5.84	2.22	15.21	13.12
5.78	18.93	38.31	6.48	31.78	60.04		6.33	4.94	8.29	8.58	8.88	18.19
22.78	31.29	10.00	16.20	63.32	38.71		8.40	2.53	5.41	10.35	15.32	11.11

Fig. 1. Thirty-minute cumulative soil-water infiltration data (in centimeters) and their spatial locations, together with tillage treatments. Distance between readings is 3 m in the east-west direction and 1.5 m in the north-south direction within tillage treatments and 3 m between adjacent tillage treatments moldboard and paraplow and chisel and no-till; 9 m separates the closets readings associated with paraplow and chisel treatments [*Cressie and Horton*, 1987].

residuals $\{r_{ijk}\}$. These residuals now appear to have come from a trend-free process (*Cressie and Horton* [1987] demonstrate lack of trend in the east-west direction) but are not homoskedastic between plots even after the square-root transformation. (As we shall see below, treatments $i = 1$ and $i = 2$ show much more error variation than treatments $i = 3$ and $i = 4$.) These residuals will be used solely to provide a good estimate of spatial correlation. Subsequent hypothesis testing will be based on the square-root data (2). If the null hypothesis of equal treatment means (of the square-root data) is accepted, this will be interpreted as inferring no "large-scale" treatment differences.

From the discussion above we can assume that

$$z_{ijk} = \mu_{ijk} + \delta_{ijk} \tag{4}$$

where μ_{ijk} is the mean of the kth observation in the jth column using treatment i and $\boldsymbol{\delta} = (\delta_{1,1,1}, \delta_{1,1,2}, \cdots, \delta_{4,3,8})'$ is a realization of a 96×1 vector of random variables with mean zero and covariance matrix $\sigma^2\Sigma$. Thus the spatial correlation among the soil-water infiltration measurements is portrayed through Σ, and in the next section this covariance structure will be estimated and modeled using geostatistical methods with the median-based residuals (equation (3)).

−2	
−2	13
−1	5589
−1	111344
−0	5555666788889
−0	000011111222233333444
0	000001111111222333334
0	5566666677789
1	00111333
1	567
2	23
2	5

Fig. 2. Stem-and-leaf plots of square-root transformed, median-swept residuals $\{r_{ijk}\}$; 0|1 denotes 0.1 $cm^{1/2}$.

3. Geostatistical Modeling of Spatial Dependence

In this section we present a brief overview of a geostatistical analysis of soil-water infiltration measurements. We assume some familiarity with geostatistical methods; a complete treatment of geostatistical methodology is given by *Journel and Huijbregts* [1978].

The spatial variability of soil-water infiltration may be characterized by the variogram [*Matheron*, 1963]

$$2\gamma(\mathbf{h}) = \text{var}\,[Z(\mathbf{s} + \mathbf{h}) - Z(\mathbf{s})] \tag{5}$$

where $\mathbf{s}$ is a vector indexing spatial location. (The semivariogram, $\gamma(\mathbf{h})$, is one half of the variogram.) That this quantity is a function only of the separation vector, $\mathbf{h}$, is part of the intrinsic hypothesis [*Matheron*, 1970]. Since the underlying variogram can never be known, it must be estimated from the data, and several such estimators are available. In the case presented here, for robustness reasons the empirical variogram was computed using the robust variogram estimator developed by *Cressie and Hawkins* [1980]. Since the data (equation (2)) do not have constant mean the median-based residuals (equation (3)) were used to estimate the variogram. Thus the empirical variogram in the east-west direction may be written

$$2\bar{\gamma}_i(2ah) = \frac{\left\{\sum_{j=1}^{3}\sum_{k=1}^{8-h} |r_{i,j,k+h} - r_{i,j,k}|^{1/2}/|N(h)|\right\}^4}{0.457 + 0.494/|N(h)|} \tag{6}$$

$$h = 1, \cdots, 7$$

where $|N(h)| = 3(8 - h)$, and $a = 1.5$ m.

Figure 3 gives plots of the empirical semivariograms for each of the treatments up to a lag distance of 15 m. Spatial dependence, as summarized by the empirical semivariograms, clearly changes with treatment. It is most pronounced for moldboard; among the four treatments, moldboard is the plowing technique that causes the greatest soil disturbance.

Semivariogram models were fitted to the robust empirical semivariograms using weighted least squares as described by

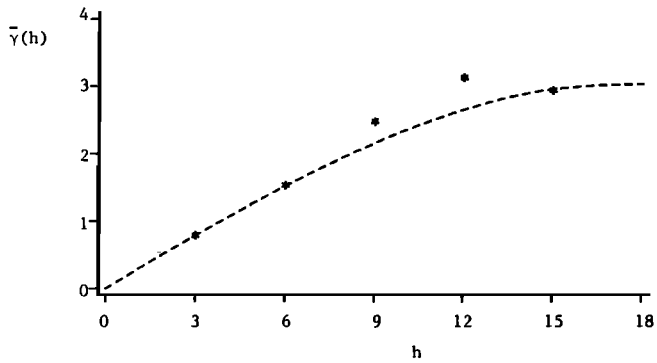

Fig. 3*a*. Robust empirical semivariogram in the east-west direction for the moldboard tillage treatment. The superimposed dashed line represents the fitted parametric semivariogram model, fitted by weighted least squares.

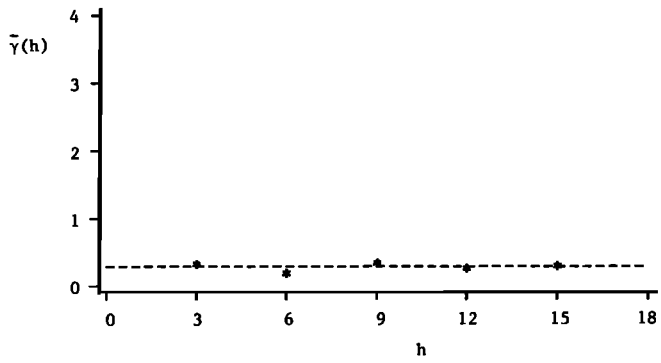

Fig. 3*c*. Robust empirical semivariogram in the east-west direction for both chisel and no-tillage treatments combined. The superimposed dashed line represents the fitted parametric semivariogram model fitted by weighted least squares.

Cressie [1985]. Since chisel and no-till semivariogram estimators were strikingly similar, they were pooled, and a semivariogram model was fit to the combined data. The following semivariogram models were fitted for the east-west direction:

Moldboard

$$\gamma_1(h) = 3.0308\left\{\left(\frac{3}{2}\right)\left(\frac{h}{17.2980}\right) - \left(\frac{1}{2}\right)\left(\frac{h}{17.2980}\right)^3\right\} \qquad 0 \le h \le 17.2980 \tag{7}$$

$$\gamma_1(h) = 3.0308 \qquad h \ge 17.2980$$

Paraplow

$$\gamma_2(h) = 0 \qquad h = 0$$
$$\gamma_2(h) = 1.6620 \qquad h > 0 \tag{8}$$

Chisel

$$\gamma_3(h) = 0 \qquad h = 0$$
$$\gamma_3(h) = 0.2881 \qquad h > 0 \tag{9}$$

No-till

$$\gamma_4(h) = 0 \qquad h = 0$$
$$\gamma_4(h) = 0.2881 \qquad h > 0 \tag{10}$$

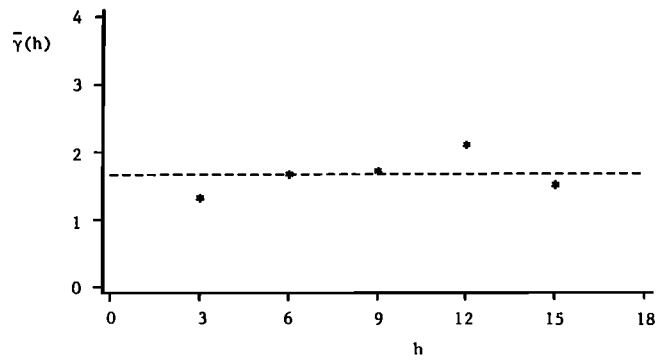

Fig. 3*b*. Robust empirical semivariogram in the east-west direction for the paraplow tillage treatment. The superimposed dashed line represents the fitted parametric semivariogram model, fitted by weighted least squares.

Figure 3 illustrates each of these models superimposed on the empirical semivariograms. Since each model has a sill $\gamma_i(\infty)$, the spatial dependence may be equally described through a stationary covariance function

$$C(h) = \sigma_i^2 - \gamma_i(h): h \ge 0 \tag{11}$$

where $\sigma_i^2 = \gamma_i(\infty)$.

Very few lags were available in the north-south direction from which to estimate the semivariograms. Those that were, justified an isotropy assumption for the spatial dependence within each plot. To examine the spatial dependence between neighboring plots, sample correlation coefficients were computed. They indicated a lack of dependence, leading to an (estimated) covariance model for Σ in (4), given by (12) below. Let the data be a realization of $\mathbf{Z}' = (\mathbf{Z}_1', \mathbf{Z}_2', \mathbf{Z}_3', \mathbf{Z}_4')$, where $\mathbf{Z}_i' = (Z_{i,1,1}, Z_{i,1,2}, \cdots, Z_{i,3,8})$. Then, our (estimated) model for the covariance structure of $\mathbf{Z}$ is

$$\text{var}(\mathbf{Z}) = \sigma^2\begin{pmatrix} \Sigma_1 & \phi & \phi & \phi \\ \phi & \Sigma_2 & \phi & \phi \\ \phi & \phi & \Sigma_3 & \phi \\ \phi & \phi & \phi & \Sigma_4 \end{pmatrix} \equiv \sigma^2\Sigma \tag{12}$$

a 96×96 block diagonal matrix where each block is 24×24. Matrices Σ_2, Σ_3, Σ_4 are proportional to the identity matrix I_{24}: $\Sigma_2 = 1.6620I_{24}$, corresponding to paraplow, and $\Sigma_3 = \Sigma_4 = 0.2881I_{24}$, corresponding to chisel and no-till. Only the matrix Σ_1, corresponding to the moldboard tillage treatment, shows spatial dependence: Σ_1 is made up of elements obtained from the stationary covariance function

$$C(h) = 3.0308 - \gamma_1(h) \tag{13}$$

where $\gamma_1(h)$ is given by (7). The notation ϕ is used to represent a matrix (of any order) with zero entries. Although two of the three variogram models correspond to no spatial dependence, there is no added difficulty in the general case of spatial correlation: Σ_2, Σ_3, and Σ_4 can be estimated in a way analogous to that of Σ_1.

The semivariogram model for the transformed moldboard data (7) was cross validated [*Stone*, 1976; *Delfiner*, 1976] using kriging. A stem-and-leaf plot of one cross-validation statistic is presented in Figure 4, and an associated normal probability plot [e.g., *Barnett*, 1975] is shown in Figure 5. Note from these diagrams that the fit of the semivariogram model is reasonable and would be quite good if it were not

3	7
2	
1	0225
0	1444667
−0	99763
−1	7222
−2	11
−3	

Fig. 4. Stem-and-leaf plot of the cross-validation statistic applied to the moldboard data; −0|9 denotes −0.9 $cm^{1/2}$.

for the extreme value of 3.70. One reason for this extreme point is that $r_{1,3,7}$ (and $z_{1,3,7}$ from (2)) is large relative to its nearest neighbors. These "spatial outliers" are hard to detect as extreme or unusual observations in a stem-and-leaf plot of the data since it ignores the (relative) spatial locations of the observations; i.e., the stem-and-leaf plot is insensitive to spatial information in the data.

As with any outlier, spatial outliers should never be deleted without good reason [*Anscombe*, 1960], although too many extreme observations will destroy even the most robust statistical analysis. Winsorization provides a compromise [see *Huber*, 1979; *Hawkins and Cressie*, 1984].

Winsorization is a data-editing technique where unusual observations are not deleted but are replaced by less extreme versions. That is, replaced z_{ijk} with

$$z_{ijk}^{(s)} = \text{med}\,\{z_{ijk}\colon k = 1, \cdots, 8\} + \hat{r}_{ijk} + c\sigma_{ijk} \qquad r_{ijk}^0 > c$$

$$z_{ijk}^{(s)} = \text{med}\,\{z_{ijk}\colon k = 1, \cdots, 8\} + r_{ijk} \qquad |r_{ijk}^0| \le c \quad (14)$$

$$z_{ijk}^{(s)} = \text{med}\,\{z_{ijk}\colon k = 1, \cdots, 8\} + \hat{r}_{ijk} - c\sigma_{ijk} \qquad r_{ijk}^o < -c$$

where $\hat{r}_{ijk}$ is the kriging predictor with kriging standard deviation σ_{ijk}, r_{ijk}^0 is the cross-validation statistic, $r_{ijk}^0 = (\hat{r}_{ijk} - r_{ijk})/\sigma_{ijk}$, and c is a tuning constant controlled by the user. Common values for c lie in the range of 1.5–3.0, the smaller the value of c, the more the data tend to be edited ($c = \infty$ corresponds to no editing at all).

Actually, if the data are Gaussian, a normal probability plot gives a nice way of obtaining c adaptively: From the probability plot, choose c to be the X coordinate of the unusual point in question, which moves the point to the target 45° line. Applying this to the spatial outlier of the moldboard data, we obtain $c = 2.04$. However, since there is some deviation about the normal line, we chose a less severe $c = 2.5$. Then $z_{1,3,7} = 6.19\ cm^{1/2}$ is replaced by $z_{1,3,7}^{(s)} = 3.99 + \{-0.5106 + (2.5)(0.7313)\} = 5.31\ cm^{1/2}$, which back on the original scale, gives $y_{1,3,7}^{(s)} = 28.22$ cm. This can be compared with $y_{1,3,7} = 38.31$ cm. After checking the experimental records, no reason for this outlier was apparent; a large subsurface crack might account for the higher than expected infiltration rate.

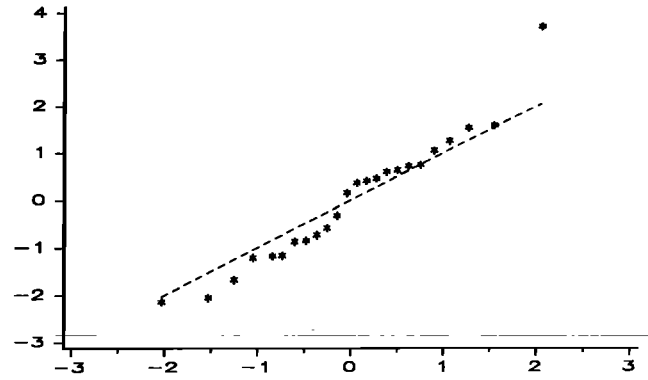

Fig. 5. Normal probability plot of cross-validation statistic. Horizontal axis denotes expected quantile; vertical axis denotes observed quantile.

In the analysis to follow the data will be edited according to the computations above, and for notational convenience we now drop the superscript "(s)." In the next section we shall proceed with inference on the mean effects $\{\mu_{ijk}\}$ of model (4). To do this we shall assume the model for var (**Z**) given by (12); however, one should not forget that it has in fact been obtained by model fitting to empirical semivariograms. Moreover, the data set is not a large one. That is why we have included in (4) a proportionality constant σ^2, to be determined by the data. The estimates of the variance and covariance parameters may be seen as the first stage of a procedure that reestimates the parameters from generalized least squares residuals; those residuals are obtained using the initial estimate of the variance matrix. *Carroll et al.* [1988] give evidence to support a small number of iterations (here 1) and an initial robust estimator of the large-scale effects (here the column medians). Although *Armstrong and Diamond* [1984], *Myers* [1985], *Kitanidis* [1986], and *Zimmerman and Cressie* [1990] have investigated the effect of parameter uncertainty on kriging, more research is needed to determine the effects of using fitted variance matrix parameters as if they were known.

4. Inference on Mean Effects

One of the goals of this paper is to formulate valid and efficient inference procedures for the mean function, μ_{ijk}, of the model in (4). On the basis of the analyses in sections 2 and 3 the following additive linear model seems appropriate:

$$Z_{ijk} = \mu + t_i + \beta_{ij} + \varepsilon_{ijk} \quad (15)$$

where

- Z_{ijk} square root of the kth datum in the jth column of treatment i;
- μ overall averages soil-water infiltration;
- t_i effect due to treatment i;
- β_{ij} effect associated with the jth column of treatment i;
- ε_{ijk} random term with zero mean and covariance matrix $\sigma^2\Sigma$ given by (12).

This model is general enough to account for north-south trend and differential treatment effects; east-west trends are assumed negligible (see section 2). Moreover, it is expressed in terms of the square-root data since the analysis of variance procedures (performed below) require an assumption of normality. Although the distribution of the data in (2) differs from that of a normal distribution, *Cressie and Whitford* [1986] have shown that analysis of variance procedures are relatively robust against long-tailed departures from normality but are not robust against departures from symmetry. With the soil-water infiltration data the square-root transformation was used to achieve the necessary symmetry. Hypotheses tested on the transformed data can be inter-

preted in terms of the model and ultimately in terms of the original question posed.

It is convenient to write the model in (15) using matrix notation:

$$\mathbf{Z} = X\boldsymbol{\beta} + \boldsymbol{\varepsilon} \tag{16}$$

where

- $\mathbf{Z}$ 96×1 data vector;
- $\mathbf{Z}$ $(Z_{1,1,1}, Z_{1,1,2}, \cdots, Z_{1,1,8}, Z_{1,2,1}, \cdots, Z_{4,3,8})'$;
- $\boldsymbol{\beta}$ $(\mu, t_1, \cdots, t_4, \beta_{1,1}, \beta_{1,2}, \beta_{1,3}, \beta_{2,1}, \cdots, \beta_{4,3})'$;
- X incidence matrix of 0's and 1's [see *Searle*, 1971, p. 145], that specifies $E(Z_{ijk}) = \mu + t_i + \beta_{ij}$;
- $\boldsymbol{\varepsilon}$ associated vector of random terms with variance matrix $\sigma^2\Sigma$ given by (12).

4.1. *Estimation of Main Effects*

The first step toward inference on $X\boldsymbol{\beta}$ is to specify an estimation procedure. If spatial dependence is ignored, or overlooked (as is often the case), the ordinary least squares estimator of $X\boldsymbol{\beta}$, namely,

$$X\hat{\boldsymbol{\beta}}_{\text{OLS}} \equiv X(X'X)^{-}X'\mathbf{Z} \tag{17}$$

(where $(X'X)^{-}$ is a generalized inverse of $X'X$; see *Rao* [1973, section 4*a*]) might be used. A stem-and-leaf plot of the ordinary least squares residuals from fitting the model (16) (with the one outlier Winsorized; see section 3) is presented in Figure 6*a*. Although the shape of this stem-and-leaf plot appears to be Gaussian, a corresponding residual plot (Figure 6*b*) shows that the variability of the residuals increases with increasing mean and thus suggests that a weighted estimation procedure is necessary.

In the case of the soil-water infiltration data, because of the heteroskedasticity and the spatial dependence, a generalized least squares estimator of $X\boldsymbol{\beta}$, namely,

$$X\hat{\boldsymbol{\beta}}_{\text{GLS}} \equiv X(X'\Sigma^{-1}X)^{-}X'\Sigma^{-1}\mathbf{Z} \tag{18}$$

is more appropriate [*Rao*, 1973, section 4*a*]. The stem-and-leaf plot of the residuals from the generalized least squares fit (Figure 7*a*) looks to be roughly Gaussian (although somewhat more granular than Figure 6*a*), and the associated residual plot (Figure 7*b*) does not suggest carrying out any further transformation or weighting. Comparing the residual plots in Figures 6*b* and 7*b*, we see that without the weighting, differences in the estimated means for each treatment are masked, whereas after the weighting the treatment divisions are more clearly defined. This is particularly true for expected values corresponding to the moldboard data (recall that plots receiving the moldboard treatment are the only ones with significant spatial dependence). In Figure 7*b* the residuals from the moldboard plots are those with the smallest expected values.

It is interesting to see how the Winsorization of the data has improved the weighted estimation of $X\boldsymbol{\beta}$. Figure 8 shows a stem-and-leaf plot of residuals obtained from the generalized least squares estimator (18) with the original (unedited) square-root data given in (2). The one very large residual of 3.23 $\text{cm}^{1/2}$ can be traced back to $y_{1,3,7} = 38.31$ cm, the same value that gave a large value for the cross-validation statistic in section 3. Residuals obtained from fitting with the unusual observation deleted (not shown here) behave very much like the residuals obtained using the edited values. However, since Winsorization uses some of the information contained in the original data point, it offers a satisfactory compromise.

24	0
22	4
20	
18	9
16	24
14	
12	1494
10	8
8	13668
6	235
4	2494557899
2	899017
0	1222455822347899
−0	8108854220
−2	97420740
−4	9964198550
−6	400
−8	77052
−10	62
−12	643
−14	82
−16	00
−18	8
−20	
−22	5

Fig. 6*a*. Stem-and-leaf plot of residuals obtained from least squares fitting of model (16) using Winsorized data. The stem 2 and corresponding leaves denote data in the interval [0.20, 0.40) $\text{cm}^{1/2}$

4.2. *A Spatial Analysis of Variance*

From the generalized least squares approach to estimation of the mean parameters in (15), we obtain a general analysis of variance in Table 1 where

$$SS_V \text{ (model)} = \hat{\boldsymbol{\beta}}'_{\text{GLS}}X'V^{-1}\mathbf{Z} - m_V \tag{19}$$

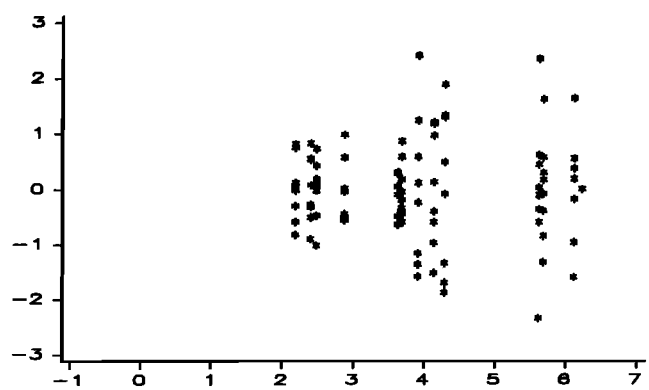

Fig. 6*b*. Residual plot (residual versus expected in $\text{cm}^{1/2}$) obtained from ordinary least squares fitting of model (15) using Winsorized data.

22	1
20	
18	226
16	11
14	14
12	11793589
10	0370
8	6
6	29
4	35833567
2	135933458
0	233899945
–0	9940998440
–2	799
–4	9616
–6	7504
–8	76520933
–10	8819640
–12	643
–14	5320
–16	8
–18	002
–20	

Fig. 7*a*. Stem-and-leaf plot for residuals obtained from generalized least squares fitting of model (16) using Winsorized data. The stem 2 and corresponding leaves denote data in the interval [0.20, 0.40) $cm^{1/2}$.

$$SS_V \text{ (columns in treatments)} = SS_V \text{ (model)} - SS_V \text{ (treatments)} \quad (20)$$

$$SS_V \text{ (residual)} = \mathbf{Z}'V^{-1}\mathbf{Z} - \hat{\boldsymbol{\beta}}'_{GLS}X'V^{-1}\mathbf{Z} \quad (21)$$

$$SS_V \text{ (corrected total)} = \mathbf{Z}'V^{-1}\mathbf{Z} - m_V \quad (22)$$

$$\hat{\boldsymbol{\beta}}_{GLS} = (X'V^{-1}X) - X'V^{-1}\mathbf{Z}$$

$$m_V = (\mathbf{1}'V^{-1}\mathbf{1})^{-}(\mathbf{Z}'V^{-1}\mathbf{1}\mathbf{1}'V^{-1}\mathbf{Z}) \quad (23)$$

V is an $N \times N$ positive-definite matrix; $\mathbf{1}$ is a $N \times 1$ vector of 1's; SS_V (treatments) is equal to an SS_V (model) type of

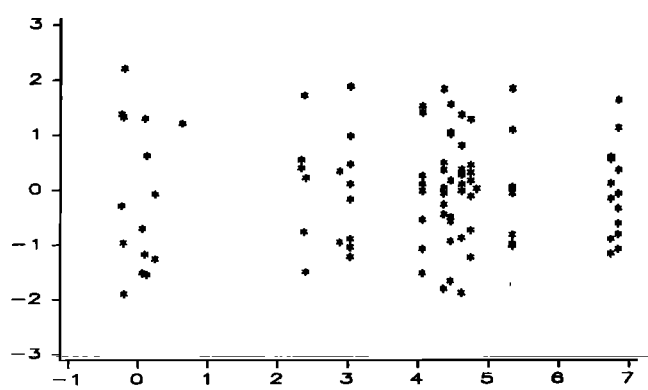

Fig. 7*b*. Residual plot (residuals versus expected in $cm^{1/2}$) obtained from generalized least squares fitting of model (15) using Winsorized data.

32	3
30	
28	
26	
24	
22	
20	
18	226
16	18
14	14
12	1278059
10	03670
8	6
6	039
4	35583567
2	35893345
0	233899945
–0	9974098440
–2	779
–4	9616
–6	7504
–8	5209933
–10	88196440
–12	43
–14	7531
–16	8
–18	6020

Fig. 8. Stem-and-leaf plot of residuals obtained from generalized least squares fitting of model (16) using unedited data. The stem 2 and corresponding leaves denote data in the interval [0.20, 0.40) $cm^{1/2}$.

expression where the model is now $Z_{ijk} = \mu + t_i + \varepsilon'_{ijk}$, fit by generalized least squares; $I(= 4)$ denotes the number of treatments, $J(= 3)$ is the number of columns within each treatment, and $N(= 96)$ is the total number of observations.

Consider now an analysis of variance (ANOVA) table for each of three models: (1) the full spatial model where $V = \sigma^2\Sigma$, given by (12); this model incorporates heteroskedasticity among the plots as well as spatial dependence; (2) the heteroskedastic model where $V = \text{diag}(\sigma^2\Sigma)$, and Σ is given by (12); this model allows only for unequal variances between plots and ignores spatial correlation; and (3) the classical model with $V = \sigma^2 I$; this model assumes independence and homoskedasticity between plots. Tables 2*a*–2*c* give the analysis of variance for each of these models.

TABLE 1. A General Analysis of Variance

Source of Variation	Degrees of Freedom	Sum of Squares
Model	$IJ - 1$	SS (model)
treatments	$I - 1$	SS (treatments)
columns in treatments	$I(J - 1)$	SS (columns in treatments)
Residual	$N - IJ$	SS (residual)
Corrected total	$N - 1$	SS (corrected total)

TABLE 2a. Analysis of Variance Associated With $Z_{ijk} = \mu + t_i + \beta_{ij} + \varepsilon_{ijk}$, for the Full Spatial Model

Source of Variation	Degrees of Freedom	Sum of Squares
Model	11	183.23
treatments	3	95.40
columns in treatments	8	87.83
Residual	84	94.12
Corrected total	95	277.35

TABLE 2c. Analysis of Variance Associated With $Z_{ijk} = \mu + t_i + \beta_{ij} + \varepsilon_{ijk}$, for the Classical Model

Source of Variation	Degrees of Freedom	Sum of Squares
Model	11	157.83
treatments	3	114.31
columns in treatments	8	43.52
Residual	84	72.83
Corrected total	95	230.66

Notice the similarity in the decomposition of the sum of squares for the heteroskedastic and classical models and the difference between these decompositions and that associated with the full spatial model. The model fitting and cross validation carried out in previous sections indicate that the full spatial model is more appropriate than the other two.

In the following sections, hypothesis tests for the parameters of the model (15) are developed. Differences between analyses based on the full spatial model and the nonspatial models will again be the most marked.

4.3. *Testing the Hypothesis of Equality of Column Means Within Treatments*

One common hypothesis frequently tested in an analysis of variance is the hypothesis of equal treatment means. However, in the spatial context this may not be a well-formulated hypothesis if there is spatial trend, i.e., if the mean depends on spatial location and is not constant from plot to plot. Thus we should check first the assumption of no spatial trend within each treatment. From (15) this amounts to checking for constant column means; specifically, test

$$H_0: \beta_{11} = \beta_{12} = \beta_{13} \tag{24a}$$

$$\beta_{21} = \beta_{22} = \beta_{23} \tag{24b}$$

$$\beta_{31} = \beta_{32} = \beta_{33} \tag{24c}$$

$$\beta_{41} = \beta_{42} = \beta_{43} \tag{24d}$$

against the general alternative (15). This hypothesis may be tested by computing the ratio

$$F = \frac{SS_V \text{ (columns in treatments)}/I(J-1)}{SS_V \text{ (residual)}/(N-IJ)} \tag{25}$$

(the sums of squares may be found in the ANOVA table) and comparing it to an F distribution on $[I(J-1), N-IJ]$ degrees of freedom. Note that if spatial correlation is present, but ignored, then an F statistic like (25), but based on ordinary least squares, does not have an F distribution.

TABLE 2b. Analysis of Variance Associated With $Z_{ijk} = \mu + t_i + \beta_{ij} + \varepsilon_{ijk}$, for the Heteroskedastic Model

Source of Variation	Degrees of Freedom	Sum of Squares
Model	11	168.16
treatments	3	115.52
columns in treatments	8	52.64
Residual	84	69.99
Corrected total	95	238.15

Computing the ratio using the appropriate values from Tables 2a–2c, we obtain $F = 9.80$ for the full spatial model, $F = 7.90$ for the heteroskedastic model, and $F = 6.27$ for the classical model.

Comparing the first of these numbers $F = 9.80$ to an F distribution (actually, the only comparison that is valid) with 8 and 84 degrees of freedom, we see that this value is significant at the 0.01 level, leading us to reject the null hypothesis of constant column means within treatments. Therefore we conclude that there is significant spatial trend.

4.4. *Testing the Hypothesis of Equality of Average Treatment Effects*

Now that the hypothesis of constant column mean within a treatment has been rejected, we can compare average treatment-plot effects by averaging over the columns within each treatment and testing the hypothesis

$$H_0: t_1 + \frac{1}{3}\sum_{j=1}^{3}\beta_{1j} = t_2 + \frac{1}{3}\sum_{j=1}^{3}\beta_{2j} = t_3 + \frac{1}{3}\sum_{j=1}^{3}\beta_{3j} = t_4 + \frac{1}{3}\sum_{j=1}^{3}\beta_{4j} \tag{26}$$

against the general alternative (15). Since average treatment effects are confounded with location, rejection of H_0 may be due to a difference in average treatment effects or may be due to a difference in spatial locations.

To test the hypothesis in (26), we refer to the general analysis of variance table at the beginning of this section and use

$$F = \frac{SS_V \text{ (treatments)}/(I-1)}{SS_V \text{ (residual)}/(N-IJ)} \tag{27}$$

Computing the ratio for the full spatial model, the heteroskedastic model and the classical model, we obtain 28.05, 44.95, and 43.95, respectively.

Notice that the values of the F ratio for the heteroskedastic and classical models are much larger than that of the full spatial model. This is because when V fails to account for the spatial correlation, SS_V (residual) is much too small. Hence the resulting F ratios (which are not F distributed) are much too large. In general, by assuming (wrongly) the classical model or the heteroskedastic model when the data are exhibiting positive spatial dependence, more frequent declarations of significant treatment differences are obtained than the data warrant.

Using the full spatial model and comparing $F = 28.05$ to an F distribution on 3 and 84 degrees of freedom, we reject the

TABLE 3. F Ratios for Testing the Hypothesis Analogous to (26) for Each of the Six Contrast Pairs

Model	Contrast					
	M-P	M-C	M-N	P-C	P-N	C-N
Full spatial	0.14	3.36	1.66	90.73	53.70	22.13
Heteroskedastic	2.00	45.66	23.29	95.67	52.99	22.13
Classical	2.22	68.70	31.88	95.67	52.99	22.13

M, P, C, N denote moldboard, paraplow, chisel, and no-till, respectively. Nominal degrees of freedom are 1 and 42, and $F^{0.05}_{1,42} \doteq 4.07$.

null hypothesis (26) and conclude that there are average treatment-plot differences.

4.5. *Pairwise Contrasts*

We now look to pairwise contrasts to determine which pairs of treatments are significantly different with regard to the amount of soil-water infiltration. Consider, for example, testing equality of average treatments effects between the moldboard and paraplow treatments. Thus test

$$H_0\colon t_1 + \frac{1}{3}\sum_{j=1}^{3} \beta_{1j} = t_2 + \frac{1}{3}\sum_{j=1}^{3} \beta_{2j} \tag{28}$$

against a general alternative, where the vector of mean-effect parameters is now

$$\boldsymbol{\beta}_{1,2} = (\mu, t_1, t_2, \beta_{1,1}, \beta_{1,2}, \beta_{1,3}, \beta_{2,1}, \beta_{2,2}, \beta_{2,3})'$$

Then using the 48×1 data vector

$$\mathbf{Z}_{1,2} = (Z_{1,1,1}, Z_{1,1,2}, \cdots, Z_{1,3,8}, Z_{2,1,1}, \cdots, Z_{2,3,8})'$$

and by notating $\operatorname{cov}(\mathbf{Z}_{1,2})$ as $\sigma^2_{1,2}\Sigma_{1,2}$, an ANOVA table with $I = 2$, $J = 3$, and $N = 48$ may be constructed. The hypothesis (28) may be tested by computing the associated F ratio (27), where the 48×48 positive definite matrix $V_{1,2}$ plays the role of V in (19) through (23).

In this case, the full spatial model corresponds to taking

$$V_{1,2} = \sigma^2_{1,2}\Sigma_{1,2} = \sigma^2_{1,2}\begin{pmatrix} \Sigma_1 & \phi \\ \phi & \Sigma_2 \end{pmatrix}$$

where Σ_1 and Σ_2 are as in (12) and $\sigma^2_{1,2}$ is a proportionality constant. The heteroskedastic model corresponds to $V_{1,2} = \operatorname{diag}(\sigma^2_{1,2}\Sigma_{1,2})$, and the classical model corresponds to $V_{1,2} = \sigma^2_{1,2}I_{48}$.

Hypotheses similar to that of (28) are considered for the other five pairs: moldboard-chisel, moldboard-notill, paraplow-chisel, paraplow-notill, and chisel-notill; the data vectors, the mean-effect parameters, and the covariance matrices are defined analogously to that of the moldboard-paraplow contrast above. Table 3 gives the associated values of (27) for each of the six contrasts and for each of the full spatial, heteroskedastic, and classical models. Recall from section 3 that the moldboard data showed the greatest spatial dependence. From Table 3 we see that the F ratios for comparison of contrasts involving moldboard using the full spatial model are much lower than those for the heteroskedastic and classical models. Consequently, if we adopted (wrongly) either a heteroskedastic or classical model in the analysis of soil-water infiltration, we would be likely to conclude significant average treatment differences, when in fact such differences are not supported by the data. Intuitively, the positive spatial correlation exhibited by the moldboard data reduces the effective number of observations, which in turn may not allow rejection of a null hypothesis involving moldboard's treatment mean with other treatment means.

Now consider the generalized least squares estimators of the treatment-plot effects, namely,

$$\hat{t}_i + \frac{1}{3}\sum_{j=1}^{3} \hat{\beta}_{ij},\ i = 1, \cdots, 4$$

computed from the elements of $\hat{\boldsymbol{\beta}}_{GLS}$ in (18). These are 2.022 $cm^{1/2}$ for moldboard, 2.478 $cm^{1/2}$ for paraplow, -0.228 $cm^{1/2}$ for chisel, and 0.494 $cm^{1/2}$ for no-till. From these estimates (as well as from the statistics in Table 3), one can see two distinct groups: moldboard-paraplow and chisel-no-till. There is not a significant treatment-plot difference between moldboard and paraplow, but there is a significant treatment-plot difference between chisel and no-till. From Table 3 and the generalized least squares estimates of treatment-plot effects, paraplow is declared the superior treatment, followed by no-till and then chisel. Although moldboard looks to be an excellent treatment, there is not enough evidence (as a result of the presence of spatial correlation) to declare it different from any of the other three treatments.

5. SUMMARY

Measurements of soil-water infiltration were used to illustrate the effects of overlooked spatial correlation. Spatial dependence was modeled using geostatistical methods, and kriging and cross validation were used to check model fit and adjust for outliers. A nested linear model with fixed effects was used as a basis for inference procedures. A spatial analysis of variance was proposed and used to test the hypothesis of large-scale trend, as well as the hypothesis of equality of average treatment effects. Because F ratios do not follow an F distribution when spatial correlation is present but overlooked, making inferences based on such ratios can lead to erroneous conclusions.

Acknowledgments. This research constitutes part of the first author's Ph.D. dissertation. It was supported in part by the National Science Foundation under grant number DMS-8703083.

REFERENCES

Anscombe, F. J., Rejection of outliers, *Technometrics*, *2*, 123–147, 1960.

Armstrong, M., and P. Diamond, Testing variograms for positive-definiteness, *Math. Geol.*, *18*, 711–728, 1984.

Barnett, V., Probability plotting methods and order statistics, *Appl. Stat.*, *24*, 95–108, 1975.

Carroll, R. J., C. F. J. Wu, and D. Ruppert, The effect of estimating weights in weighted least squares, *J. Am. Stat. Assoc.*, *83*, 1045–1054, 1988.

Cressie, N., Fitting variogram models by weighted least squares, *Math. Geol.*, *17*, 563–586, 1985.

Cressie, N., and D. M. Hawkins, Robust estimation of the variogram, I, *Math. Geol.*, *12*, 115–125, 1980.

Cressie, N. A. C., and R. Horton, A robust-resistant spatial analysis of soil water infiltration, *Water Resour. Res.*, *23*, 911–917, 1987.

Cressie, N., and H. J. Whitford, How to use the two-sample *t*-test, *Biometrical J.*, *28*, 131–148, 1986.

Delfiner, P., Linear estimation of nonstationary spatial phenomena, in *Advanced Geostatistics in the Mining Industry*, edited by M. Guarascio et al., pp. 49–68, D. Reidel, Hingham, Mass., 1976.

Hawkins, D. M., and N. Cressie, Robust kriging—A proposal, *Math. Geol.*, *16*, 3–18, 1984.

Huber, P. J., Robust smoothing, *Robustness in Statistics*, edited by R. L. Launer and G. N. Wilkinson, pp. 34–45, Academic, San Diego, Calif., 1979.

Journel, A. G., and C. J. Huijbregts, *Mining Geostatistics*, Academic, San Diego, Calif., 1978.

Kitanidis, P. K., Parametric uncertainty in estimation of spatial functions: Bayesian analysis, *Water Resour. Res.*, *22*, 499–507, 1986.

Matheron, G., Principles of geostatistics, *Econ. Geol.*, *58*, 1246–1266, 1963.

Matheron, G., The theory of regionalized variables and its applications, *Cah. 5*, Cent. de Morphol. Math., Ecole des Mines de Paris, 1970.

Mukhtar, S., J. L. Baker, R. Horton, and D. C. Erbach, Soil water infiltration as effected by the use of the paraplow, *Trans. ASAE*, *28*, 1811–1816, 1985.

Myers, D. E., Some aspects of robustness, *Sci. Terre, Ser. Inf. Geol. 24*, 63–79, 1985.

Rao, C. R., *Linear Statistical Inference and Its Applications*, John Wiley, New York, 1973.

Searle, S. R., *Linear Models*, John Wiley, New York, 1971.

Stone, M., Cross-validatory choice and assessment of statistical prediction, *J. R. Stat. Soc., Ser. B.*, 114–147, 1976.

Zimmerman, D. L., and N. Cressie, Mean-squared prediction error in the spatial linear model with estimated covariance parameters, *Ann. Inst. Stat. Math.*, in press, 1990.

N. A. C. Cressie, Department of Statistics, Iowa State University, Ames, IA 50011.

C. A. Gotway, Division 7223, Sandia National Laboratory, P. O. Box 5800, Albuquerque, NM 87185.

(Received July 31, 1989;
revised June 18, 1990;
accepted July 10, 1990.)